

Stress reduction in push belt rings using residual stresses

An approach towards increased power density for push belt CVT's

Ir. F. van der Sluis, Ir. A. Brandsma, Ing. J. van Lith, Ing. K. van der Meer,
Ir. A. van der Velde, Ir. B. Pennings, Van Doorne's Transmissie b.v., Bosch Group, Tilburg



Summary

Since the push belt CVT first came into production, customer specifications on transmittable power, torque, space envelope, ratio coverage and durability have been extended. In answer to these changing demands, Van Doorne's Transmissie (VDT) dedicates itself to a continuous effort to improve the power density of its push belt.

Power density can be increased by reduction of critical stress levels in the rings of the belt. Within the current belt interface this is realised by improved pre-bending.

Rings are pre-bent in production. The process introduces a residual stress profile in the ring that helps to lower stress levels in critical areas during operation in the variator. Ring load analysis indicates that further improvement of the pre-bend process is possible.

This paper describes a theoretical model that helps to understand the stress critical areas in the rings that can be influenced by the pre-bend process. Theory is checked with experimental results revealing that model and test are consistent. Improvements have been implemented in the new push belt design to increase the power density of CVT applications.

1. Introduction

Over the last years the CVT market has seen a sharp increase in the number of applications. For the year 2002 numbers are foreseen to double. At this moment most car manufacturers have a car with CVT in their program or are working to get there.

For VDT, the main supplier of steel push belts, this increase in demand means a tremendous effort. In order to keep pace, large steps in production numbers are scheduled leading to a production increase of 590,000 units in the year 2001 towards 1,200,000 units in the year 2002. Together with the increase in numbers also an increase in application range is noticed. To reduce the level in transmission diversity, customer requirements regarding transmittable power, torque, space envelope, ratio coverage and durability are becoming more severe. In meeting those requirements, power density of the belt needs to be extended beyond the current state of the art belt design. To enable this at short notice, solutions have to be found within the current belt interface.

Power density of a steel push belt mainly is determined by the fatigue limit of the ring material [1]. To secure belt durability, ring stress must not exceed a certain level. An increase of power density without a ring stress increase can be achieved by changes in geometry.

Next to pure tension, bending plays an important role in the sum of stresses working on the rings. Bending stress levels can form up to 40% of the stress level induced during maximum load situations in the variator. They result from the radii the belt encounters in the variator and therefore are largest at the minimum running radii in the ratios Low and Overdrive.

Stresses from bending can also be brought into the ring during production before it is subjected to loads in the variator. This so-called residual stress, resulting from plastic deformation of the ring, can help to reduce the stress levels in critical areas during operation in the variator.

2. Introduction of residual stresses in push belt rings during production

After the basic ring is formed during the successive production steps pipe-rolling, welding, pipe-slitting, deburring and rolling, all previously introduced stresses are removed by annealing the ring. Then residual stresses are brought into the ring by means of three processes:

1. Calibration or pre-bend process : Brings the ring to a correct (calibration) length.
2. Hardening process : Increases the yield and fatigue limit of the material.
3. Nitriding process : Increases the wear resistance of the ring surfaces.

All processes can be optimised by adjustment of process parameters. This paper focuses on the optimisation of the pre-bend process of which **figure 1** shows a schematic view.

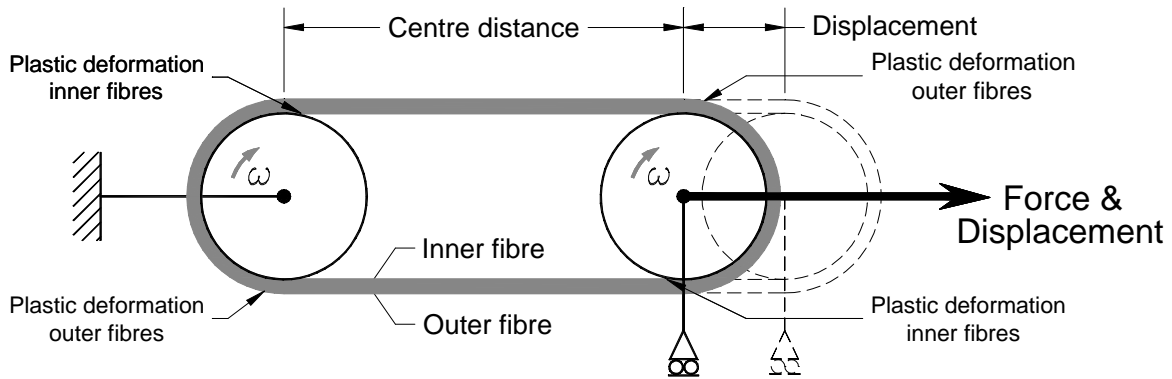


Fig. 1: Calibration or pre-bend process: calibration length definition and mechanical residual stress introduction.

During the pre-bend process the ring is elongated to a correct length. At the straight parts the ring is under tension. At the rollers the ring is bent and an additional stress is introduced. During a centre distance increase of the rollers the ring material is stressed beyond its yield limit and deformation becomes plastic.

Plastic deformation starts at the surface fibres when the ring goes from straight to roller radius and vice versa. During ring elongation, plastic deformation runs up to the neutral line. The stress profiles based on ideal plastic material behaviour are shown in **figure 2**.

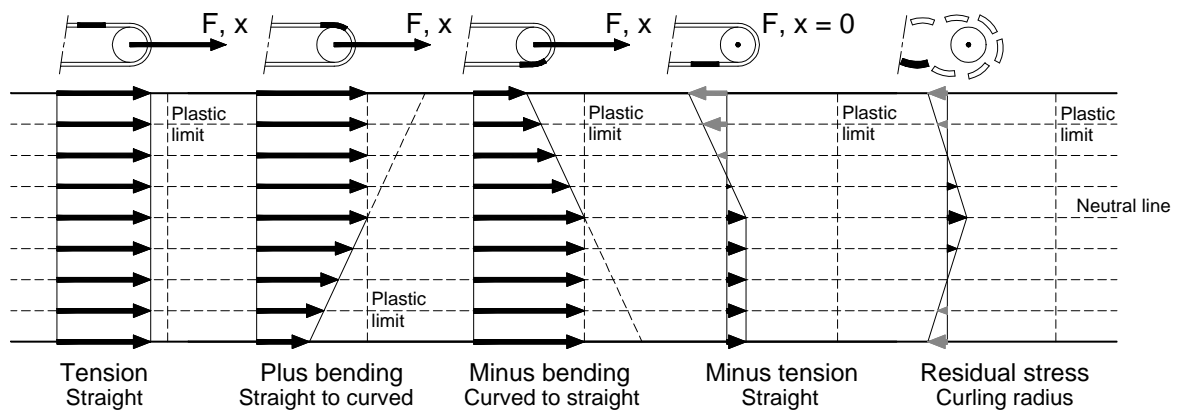


Fig. 2: Ring stress profiles during the pre-bend process. Input for the process is the annealed (stress-free) ring.

After the process a bending moment is left in the ring. This can be seen in case a ring part is cut free from the ring and curls up to a certain radius called the curling radius. In this situation the resulting bending moment from residual stresses on the ring part is zero and the residual stress profile resembles the last stress profile in figure 2. The cross-section contains compressive stress at the inner and outer fibre and tension stress at the neutral line.

In case the ring is bent straight the required bending moment leads to the fore last stress profile in figure 2.

3. Optimum residual stress profile

During operation in the variator the ring with curling radius is subjected to stresses from bending. Most critical load cases concerning bending are:

1. Bending the ring straight causing maximum tension at the inner ring fibres.
2. Bending the ring to its minimum running radius causing maximum tension at the outer ring fibres.

Figure 3 shows these load cases starting with the curling radius containing residual stresses from pre-bending. Only stresses from bending the ring are reviewed.

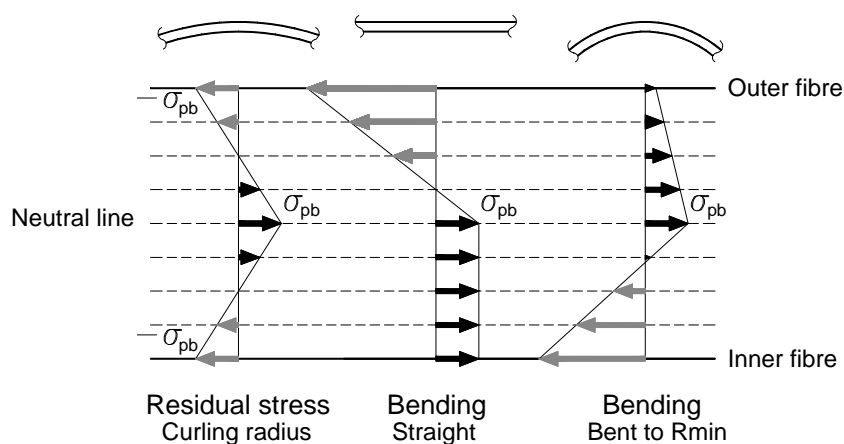


Fig. 3: Ring stress profiles in variator during critical load cases. Not optimal situation, only bending included. Hardening/nitriding excluded.

The stress profiles have maximum values at the inner, outer and neutral fibre. The tension stress at the neutral line is not influenced by bending and thus is determined by the pre-bend process. It is the maximum level of residual stress denoted by σ_{pb} .

Bending of straight beams can be described using simple beam theory. Maximum stress in longitudinal direction σ and bending moment M are calculated using the following equations:

$$\mathbf{s} = \frac{\mathbf{d} \cdot E}{R} \quad (1)$$

$$M = \frac{E \cdot I}{R}$$

Where:

- δ = Maximum fibre distance from neutral line [mm]
- R = Bending radius neutral line [mm]
- E = Young's modulus of elasticity [N/mm²]
- I = Moment of inertia beam cross-section [mm⁴]

For curved rings, equations (1) can be used as an approximation. The curling and bending radii of the rings are sufficiently large compared to their maximum fibre distance to allow this. Stress deviations lie below 0.2%. A more accurate calculation method is found in [2].

The curling radius R_{curl} determines the stress profile in a straightened ring part. To bend the ring straight, a bending moment applying a maximum stress level σ_{bs} is required:

$$\mathbf{s}_{bs} = \frac{\mathbf{d} \cdot E}{R_{curl}} \quad (2)$$

At the minimum running radius for the ring in the variator, denoted by R_{min} , the ring is subjected to a bending moment in the opposite direction. The maximum stress σ_{bmax} occurring while bending an initially straight ring part to this minimum running radius is:

$$\mathbf{s}_{bmax} = \frac{\mathbf{d} \cdot E}{R_{min}} \quad (3)$$

For tension stress minimisation it is desirable that maximum tension stress at the inner fibre (at straight part) equals maximum tension stress at the outer fibre (at minimum running radius). This means:

$$-\mathbf{s}_{pb} + \mathbf{s}_{bs} = -\mathbf{s}_{pb} - \mathbf{s}_{bs} + \mathbf{s}_{bmax} \quad (4)$$

Or:

$$-s_{pb} + \frac{d \cdot E}{R_{curl}} = -s_{pb} - \frac{d \cdot E}{R_{curl}} + \frac{d \cdot E}{R_{min}} \quad (5)$$

Which leads to:

$$R_{curl} = f_{pb} \cdot R_{min} \quad \text{where, } f_{pb} = 2 [-] \quad (6)$$

The theoretical optimal pre-bend factor $f_{pb} = 2$ is the basis for the pre-bend process. For rings with optimum curling radius, stress profiles now look like **figure 4**. Both bending the ring straight and bending the ring to the minimum running radius lead to identical but mirrored stress profiles.

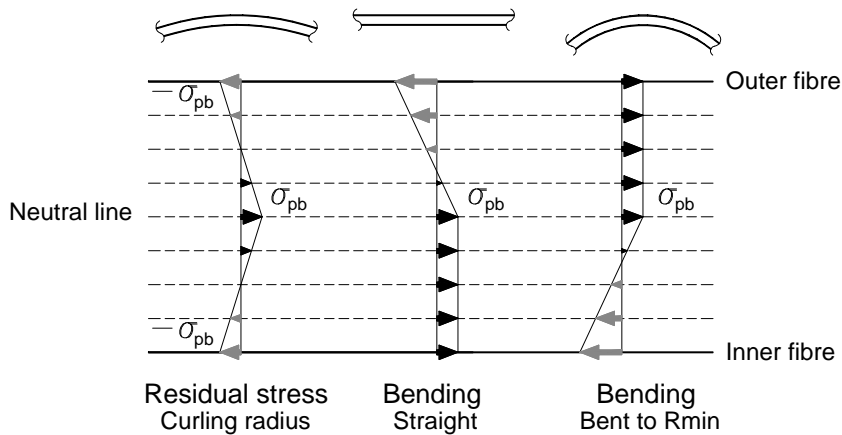


Fig. 4: Ring stress profiles in variator during critical load cases. Optimal situation, only bending included. Hardening/nitriding excluded.

4. Influences from subsequent production processes

After pre-bending, the hardening and nitriding process influence the residual stress profile in the ring leading to a different curling radius than obtained from the pre-bend process. It is shown equation (6) remains valid as long as the rings resulting from these processes answer to the optimum curling radius.

Hardening and nitriding cause relaxation in the ring material. During relaxation, the initial residual stress level in the material decreases with a certain factor. This factor depends on process time, process temperature and initial residual stress as shown in **figure 5**.

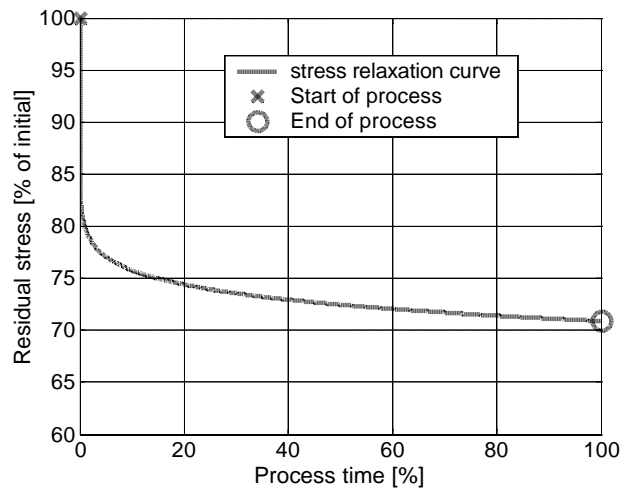


Fig. 5: Residual stress relaxation during a (constant) high temperature process (example from literature [3]).

As process time and temperature preferably are equal for all rings, the final factor mainly is a function of the initial residual stress level introduced by pre-bending.

During nitriding, compression stress is brought into a thin surface layer of the material. This stress is balanced by a tension stress working on the material in the centre as shown in **figure 6**.

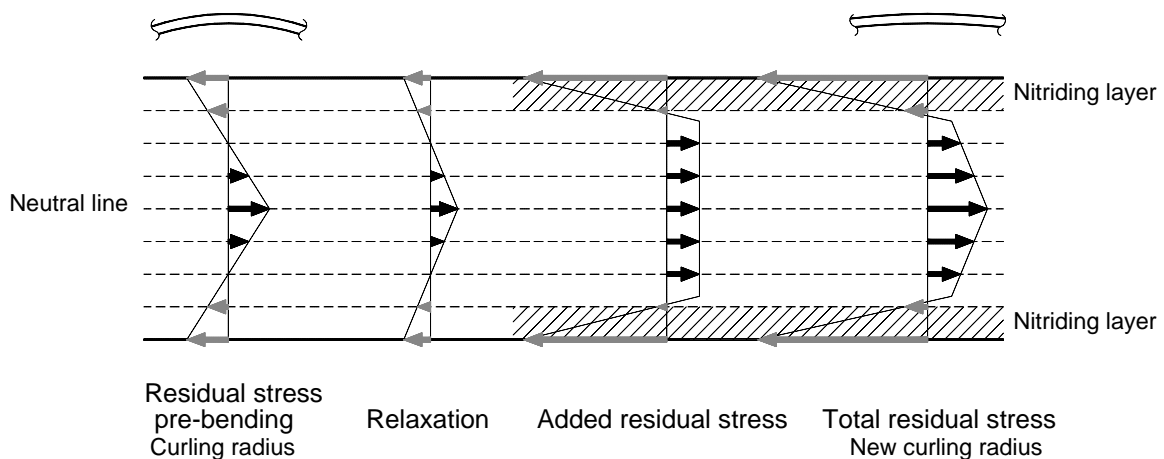


Fig. 6: Influences hardening and nitriding process on residual stress for a free ring part.

The relaxation of mechanical residual stress during hardening and nitriding causes curling radii originating from pre-bending to increase.

The symmetrical residual stress profile added by nitriding does not influence equation (6). It falls out of equation (4) because of its symmetry.

The maximum ring stress level occurring during operation in the variator is influenced by relaxation. Optimal combinations of pre-bending and relaxation result in optimal curling radii. Consequently the bending moments on the ring for bending straight and bending to the minimum radius cause identical maximum stress levels past the nitriding layer for both sides of the ring. This optimal situation is shown in **figure 7**. Stresses at the surface remain compressive as a result from the nitriding layer. The largest tension stresses occur between the nitriding layers.

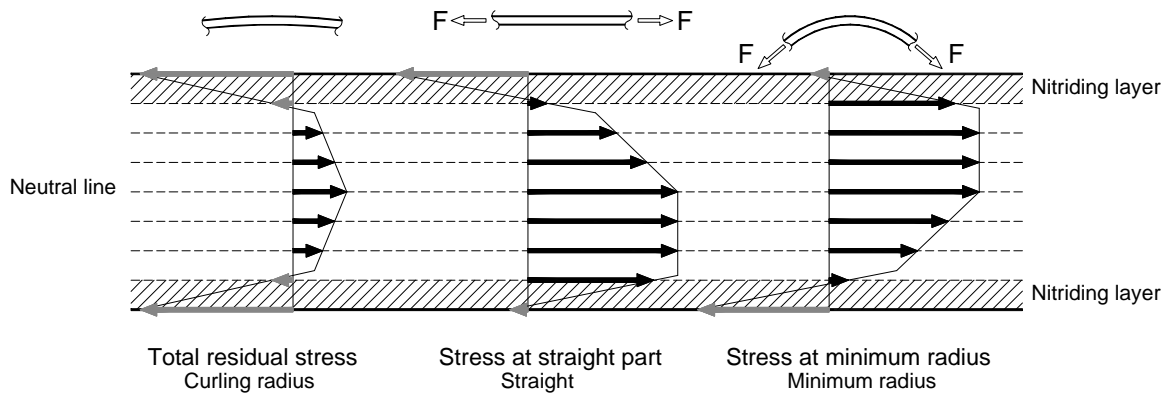


Fig. 7: Ring stress profiles in the variator, bending and tension included. Hardening/nitriding included.

For present commercial belt applications, the production settings for pre-bending, hardening and nitriding aim to generate rings of which the final curling radii answer to the optimum pre-bend factor $f_{pb} = 2$. In this case the bending moment required for bending the hardened and nitrided ring straight equals the bending moment for bending the ring to its minimum running radius and maximum and minimum stresses for all symmetrically located fibres are equal.

5. Additional effects and model adaptation

Theory as discussed until now points towards the following equation to obtain equal stresses at the inner and outer ring fibres:

$$R_{curl} = 2 \cdot R_{min} \quad (7)$$

Up to this point however a limited number of influences has been taken into account:

1. Pre-bend process (mechanical residual stress introduction).
2. Relaxation and nitriding process (additional residual stress influence).
3. Bending of rings with rectangular cross-sections based on simple beam theory.

The focus of these influences has been laid on stress levels in the longitudinal direction using a one-dimensional analysis. In practice the following phenomena will have an additional effect on the stress level in the ring. Some of them require a two- or even a three-dimensional analysis.

1. Contact between element and inner ring
2. Crowning radius of the ring in transverse direction
3. Anticlastic effect leading to cross-section variations during bending

These phenomena are discussed below.

5.1. Contact between elements and inner ring

When the inner ring is at the pulley, its overall running radius is locally disturbed by the actual surface the ring is in contact with. This surface made up out of elements forms a polygon surface as illustrated in **figure 8**. It influences the stress profile in the ring by the following two effects:

- Contact stress in the local contact point between ring and element.
- Additional stress from local bending.

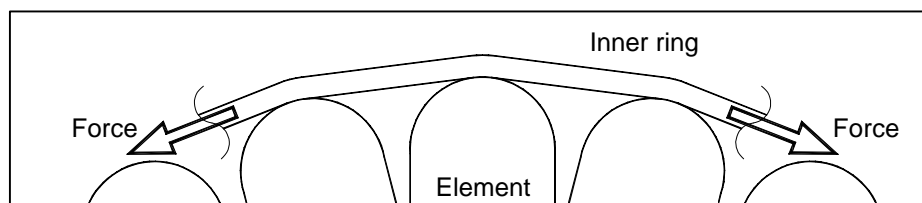


Fig. 8: Contact between element and ring: polygon effect. (Figure is not on scale).

Contact stresses occur at the inner radius of the inner ring where the ring is in contact with the elements. In the contact friction occurs resulting from the ring sliding over the elements.

The element - ring contact can also lead to additional local stresses from bending in the ring. As the ring follows the local contact geometry, it experiences a smaller bending radius than the overall running radius. This causes increased compression stress at the inner fibre and increased tension stress at the outer fibre of the ring. In theory also local straightening of the ring can occur between two elements as can be seen in figure 8.

At the straight part between the pulleys the effect is not present. Stress amplitudes between the situations straight (not on pulley) and bent (on pulley) therefore will increase for inner and outer fibre.

The possibilities for stress reduction by means of measures in the element - ring contact fall outside the scope of this paper. The subject remains an important research item.

5.2. Crowning

After production the ring is not flat in the transverse direction. This effect is referred to as crowning. The surface curvature is approximated with a radius R_{crown} as defined in **figure 9**.

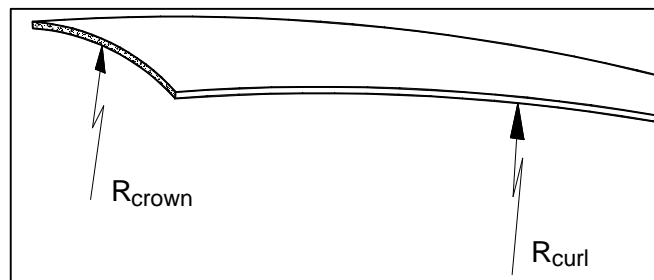


Fig. 9: Definition crowning radius.

For small crowning radii, the cross-section of the ring can no longer be considered rectangular. **Figure 10** shows increasing maximum fibre distances for crowned rings. The changing fibre distances lead to a different moment of inertia. As the cross-section no longer is symmetrical around the horizontal neutral line, the minimum moment of resistance W is different for inner and outer fibre. This can be seen in **figure 11**.

At the pulley the ring experiences a pre-determined bending radius. The bending moment depends on bending radius and moment of inertia according equation (1). Fibre distances and bending radius determine the stress levels in the ring. The increased fibre distances lead to higher stresses for crowned cross-sections in comparison to rectangular cross-sections.

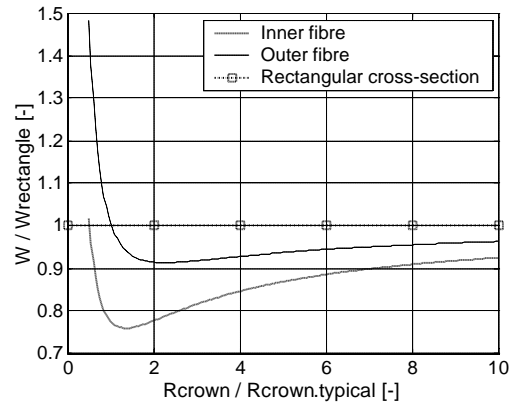
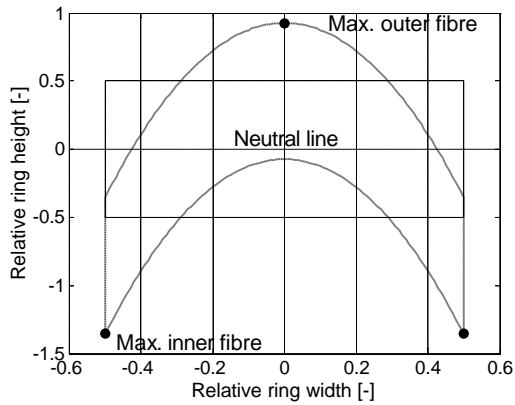


Fig. 10: Ring contour rectangular versus crowned cross-section.

Fig. 11: Relative minimum moment of resistance for inner and outer fibre as a function of crowning radius.

From **figure 12** the ultimate strains in longitudinal direction can be derived based on simple beam theory. For the moment an initially straight beam with crowned cross-section bent at a radius R is assumed.

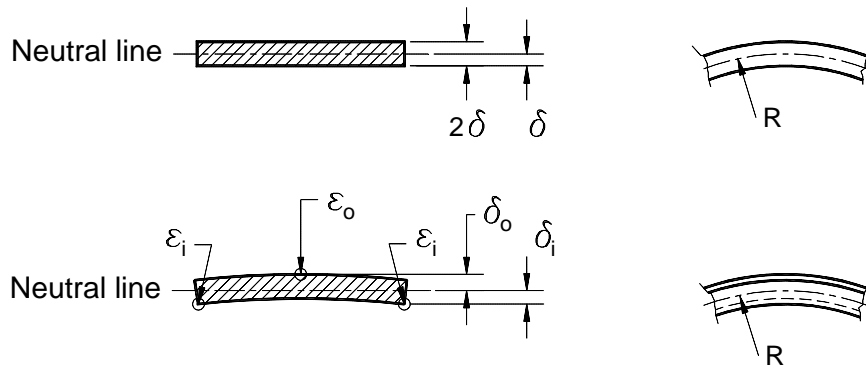


Fig. 12: Rectangular and crowned cross-section bent at radius R.

The equations for the ultimate strains in the crowned cross-section are:

$$e_i = \frac{-d_i}{R} \tag{8}$$

$$e_o = \frac{d_o}{R} \tag{9}$$

Where:

$\delta_{i,o}$ = maximum fibre distance at inner and outer surface [mm]

$\epsilon_{i,o}$ = longitudinal strain at inner and outer maximum fibre distance [-]

Equation (5) can now be rewritten. Again the condition of equal maximum tension stress for inner and outer surface is used. Under the assumption that the residual stress is σ_{pb} at both locations, the equation becomes:

$$-s_{pb} + \frac{d_i \cdot E}{R_{curl}} = -s_{pb} - \frac{d_o \cdot E}{R_{curl}} + \frac{d_o \cdot E}{R_{min}} \quad (10)$$

From this equation the pre-bend factor f_{pb} can be derived:

$$R_{curl} = \frac{d_i + d_o}{d_o} \cdot R_{min} \quad (11)$$

$$f_{pb} = \frac{d_i + d_o}{d_o} \quad (12)$$

For a rectangular cross-section where $\delta_i = \delta_o$, the pre-bend factor f_{pb} is 2. For crowned cross-sections the factor depends on crowning radius and ring geometry. **Figure 13** shows equation (12) as a function of crowning radius for a typical ring geometry.

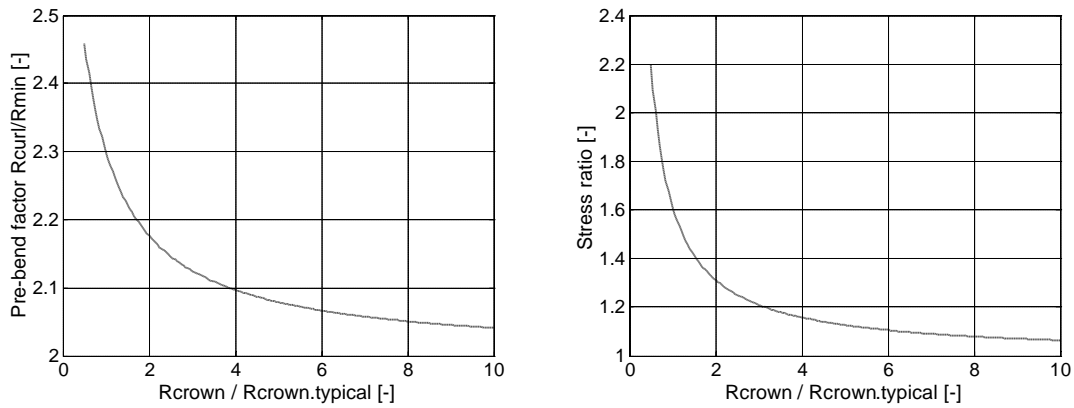


Fig. 13: Pre-bend factor f_{pb} as a function of crowning radius for a typical ring geometry.

Fig. 14: Stress ratio between a crowned and a rectangular cross-section as a function of crowning radius for the optimum pre-bend factors of figure 13. Only crowning is reviewed!

At this point stress increases caused by crowning of the ring can be estimated. **Figure 14** shows tension stress ratios between a rectangular and a crowned cross-section as a function of relative crowning radius for the typical ring geometry of figure 13.

For certain curling and crowning radius combinations with optimal pre-bend factor, stresses can be further minimised by increasing the crowning radius. In case an optimum pre-bend factor is maintained this leads to a decreasing curling radius.

It can be concluded that crowning influences the stress levels from bending in the rings and therefore directly affects the optimum curling radius. Larger crowning radii result in lower stress and smaller optimum curling radii. Crowning leads to pre-bend factors larger than 2.

5.3. Anticlastic effect

In case a ring with a curling radius and a crowning radius is bent, crowning changes. During bending straight the radius R_{crown} decreases and crowning becomes worse. During bending at a smaller radius than the curling radius, R_{crown} increases and crowning reduces. This behaviour, illustrated in **figure 15**, can be explained by the anticlastic effect.

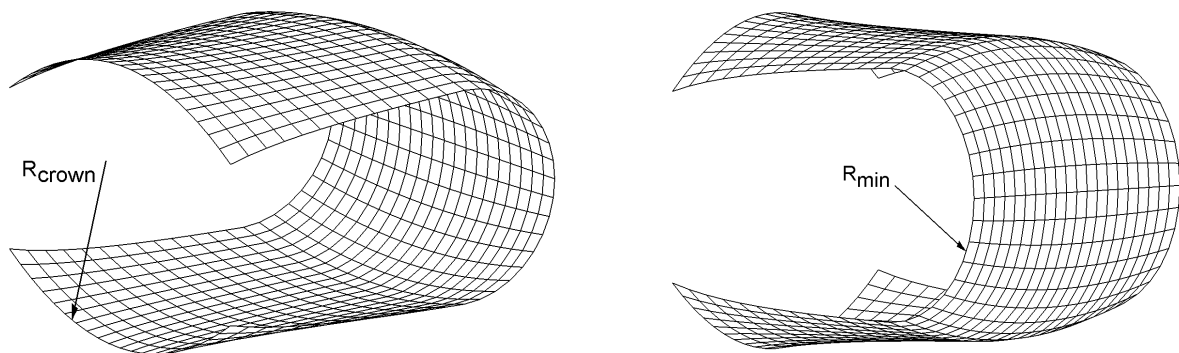


Fig. 15: Varying crowning radius during bending and straightening.

This effect, caused by transverse contraction, introduces crowning changes during bending. The effect is described in literature for straight plates with a rectangular cross-section [4]. Also described here are the differences in stresses on the surface for anticlastic theory and simple beam theory. The ratio between these two is given for a rectangular cross-section in **figure 16**. Shown are the ratios for tension and for compression stress, both in longitudinal direction.

Typically tension stress increases at the edges of the ring. Compression stress decreases at these locations.

Figure 17 shows the deflection of the neutral line for the initially rectangular cross-section.

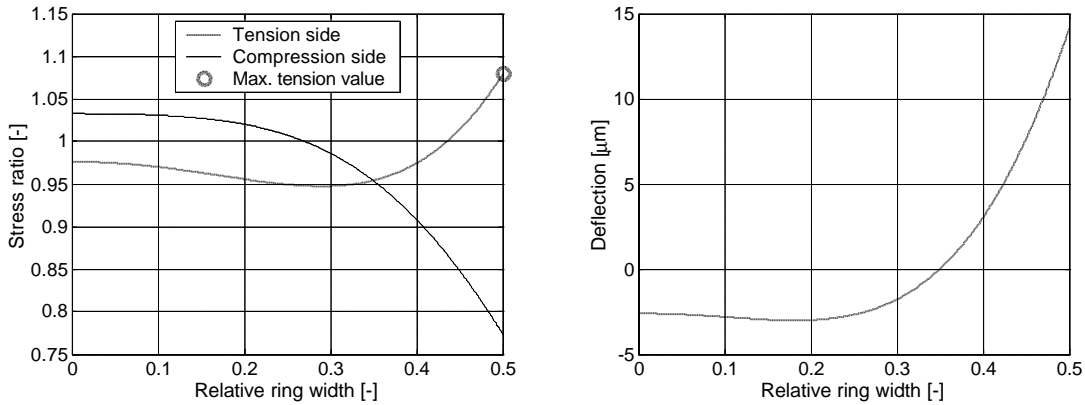


Fig. 16: Stress ratio anticlastic versus beam theory for a typical rectangular cross-section bent at $R = 30$ [mm].

Fig. 17: Anticlastic ring deflection for a typical rectangular cross-section bent at $R = 30$ [mm].

Clearly crowning radius and stress are influenced by the anticlastic effect. The effect can be introduced for crowned rings using two factors applicable for the locations of interest. This extends equation (10) as follows:

$$-s_{pb} + f_i \cdot \left(\frac{d_i \cdot E}{R_{curl}} \right) = -s_{pb} - f_o \cdot \left(\frac{d_o \cdot E}{R_{curl}} - \frac{d_o \cdot E}{R_{min}} \right) \quad (13)$$

Where:

f_i = stress factor anticlastic effect, maximally loaded inner fibre during straightening [-].

f_o = stress factor anticlastic effect, maximally loaded outer fibre during bending [-].

With the introduction of these factors the assumption of simple beam theory is left. Changes in maximum fibre distances, caused by deforming cross-sections and varying neutral lines, are now included.

The factor f_i is applicable for the edges of a ring with crowned cross-section. Tension will be maximal here because fibre distances are maximal. The factor f_o is applicable for the middle of the ring for the same reason.

From equation (13) follows:

$$R_{curl} = \frac{f_i \cdot d_i + f_o \cdot d_o}{f_o \cdot d_o} \cdot R_{min} \quad (14)$$

To investigate the factors f_i and f_o , three-dimensional Finite Element Method (FEM) calculations were performed with varying parameters R_{min} , R_{crown} and R_{curl} . Anticlastic effects were included. **Figure 18** and **figure 19** show some results for identical curling radius and two different crowning radii. Tension stresses from FEM analysis are compared with tension stresses calculated with equation (10) in which anticlastic effects are not included.

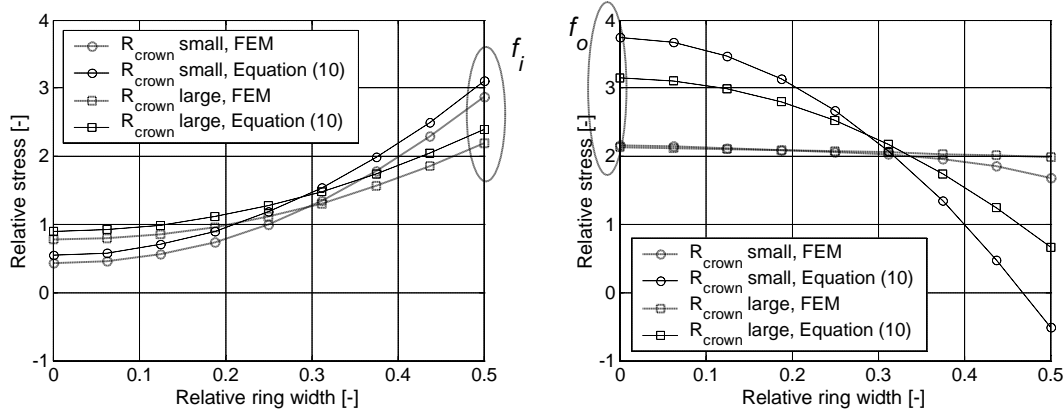


Fig. 18: Stress results longitudinal direction, inner surface during **bending straight**.

Fig. 19: Stress results longitudinal direction, outer surface during **bending to a minimum radius**.

The influence of anticlastic deflections on stresses during straightening of the ring is relatively small as can be seen in figure 18. The influence of anticlastic deflections on stresses during bending to the minimum radius is much larger. Figure 19 shows that the stress increase caused by crowning is partly undone by the anticlastic effect.

Figures 18 and 19 show that maximum tension stresses still can be found at the inner surface edges for rings bent straight and at the outer surface middle for rings bent to a smaller radius.

Comparison of results from FEM analysis and equation (10) learns that in the considered typical ranges for crowning, curling and bending radii the factor f_i is rather independent on crowning radius. Factor f_o is dependent on crowning radius. FEM analysis shows that both factors depend on curling radius in the same degree, which also can be recognised in **figure 20**. It leads to the conclusion that f_i/f_o merely is dependent on crowning radius.

The factor f_o and thus f_i/f_o is practically independent on the minimum bending radius R_{min} . Variations of R_{min} within its typical range show no significant differences. This is in accordance with literature [4]. Figure 20 contains an example of an increased minimum bending radius.

Knowing this, we can write:

$$f_{pb} = \frac{\left(\frac{f_i}{f_o}\right) \cdot d_i + d_o}{d_o} \quad (15)$$

For a typical ring geometry the factor f_i/f_o by approximation is linearly dependent on the reciprocal of the crowning radius. This is depicted in figure 20.

Note that the anticlastic effect can cause a shift in the location of maximum tension stress for larger crowning radii. The approach above where it is assumed that the maximum tension stress lies in the middle of the ring (figure 19) is then no longer valid. For a rectangular ring cross-section for instance, the location of maximum stress during bending does not lie in the middle. It lies at the edges as shown in figure 16.

The range of crowning radii where the maximum tension stress from bending remains located in the middle of the ring however lies within the typical range of crowning radii. Equation (15) is an acceptable approximation here.

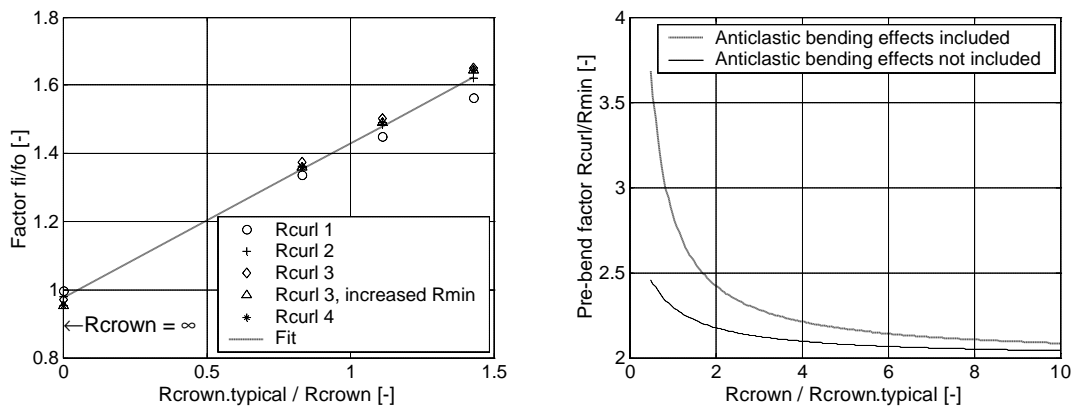


Fig. 20: FEM analysis results: factor f_i/f_o as a function of inverse crowning radius for a typical ring geometry.

Fig. 21: Approximation pre-bend factor f_{pb} as a function of crowning radius, anticlastic effects included.

Figure 21 shows equation (15) for a typical ring geometry. Also the pre-bend factor f_{pb} without anticlastic influences from equation (12) is included.

It is concluded that the anticlastic effect influences tension stresses in a crowned ring. FEM analysis shows that the one-dimensional model presented in the previous section is allowed in case a multiplication factor is included describing the influences of the anticlastic effect. This factor mainly brings a reduction of tension stresses at the outer fibre into account, estimated too high by the one-dimensional model. The anticlastic effect results in larger optimum curling radii.

6. Test definition

Tests on rings with the current process settings show that for belt failures caused by ring fatigue, fracture initiation predominantly occurs at the inner radius of the inner ring in the belt. As shown, curling radius, crowning radius and element - ring interaction influence the inner fibre load. With the latter falling outside the scope of this investigation a test is done with changed curling and crowning radii.

To validate the described curling and crowning radius influences, tests with two belt types have run. Tested are the 24/9 belt type with 24 mm element width and 2×9 rings and the 30/12 belt type with 30 mm element width and 2×12 rings.

The settings for the rings are drawn in **figure 22** and **figure 23**. To approach the optimum settings described by theory, the new settings should result in increased curling and/or crowning radii. For production reasons it was not possible to reach an exact optimum.

Note that due to geometrical differences between the two belt types the curves defining the optimum pre-bend factor are not equal.

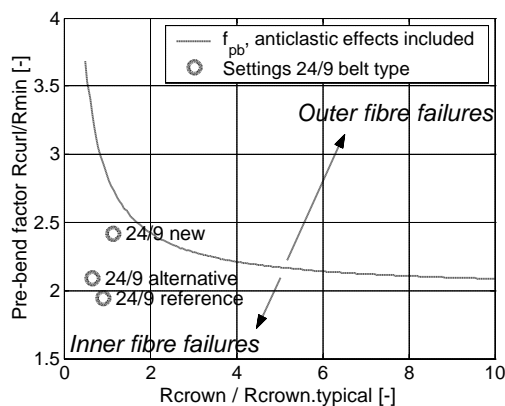


Fig. 22: Settings test data 24/9 belt application.

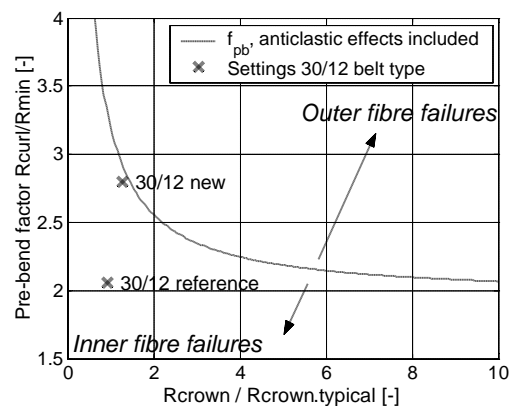


Fig. 23: Settings test data 30/12 belt application.

All belts were tested using an Overload Fatigue Test (OFT). This is a single ratio test on variator level during which belt and variator are tested in a belt box powered by an electric motor. It is an advanced-stress test designed to obtain life-testing data within a reasonable short period. During the test the belt is overloaded above the full load settings that occur during operation in a vehicle and which are normally applicable for Long Durability Cycle (LDC) belt box tests.

During an OFT both speed and torque are increased beyond the full load level. The variator ratio is adjusted to obtain a small running radius at the driven pulley. The clamping force is increased to maintain a normal safety. The belt is tested until ring fracture occurs which is detected using a fracture detection method.

7. Test results

The test results are shown using a Weibull plot in **figure 24** and **figure 25**. Figure 24 shows the results for the 24/9-belt application. Figure 25 shows the results for the 30/12-belt application.

For both belt types the rings with the new settings show increased life with a factor that lies around 1.7.

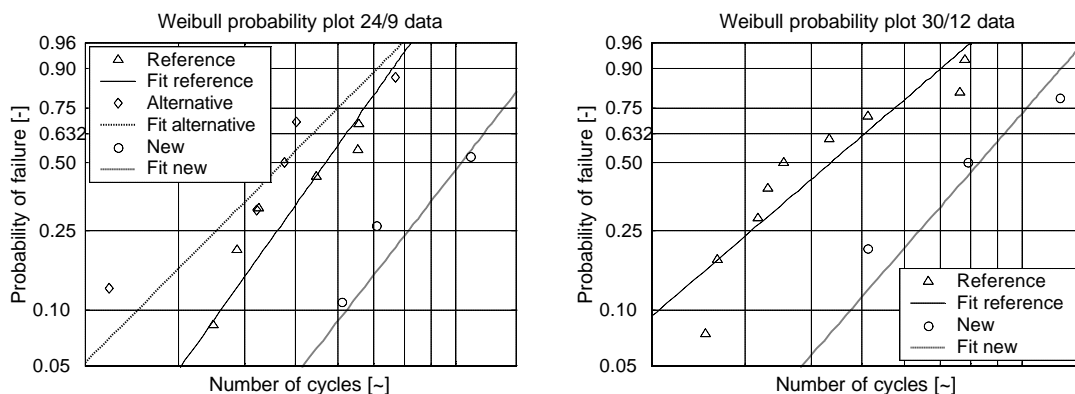


Fig. 24: Test results for 24/9 belt type data.

Fig. 25: Test results for 30/12 belt type data.

The 24/9 belts with rings produced using the alternative setting with reduced crowning radius show a slight decrease in life. All results indicate that the hypothesis of improved life for a more optimal combination of crowning and curling radius can be accepted.

For some of the new 30/12 belts crack initiation was found to lie in the middle of the outer surface of the inner ring, supporting the theory presented in this paper.

8. Implementation in CVT applications

Based on the discussed effects, power density of the push belt CVT can be further improved by using increased crowning and/or curling radii. The new process settings are used in the new belt design and lead to a crowning and curling radius increase of about 25% compared with the current belt design.

At this moment VDT is carrying out validation tests for 5 different car/transmission manufacturers from Japan, Europe and the U.S.A. to secure the introduction of the new belt design into new CVT applications. Production for these applications starts in 2002, 2003 and 2004 respectively.

The first new application equipped with the new belt design is the Nissan Murano. The Nissan Murano has been introduced to the world at the New York International Autoshow in spring 2002 and will be available in October 2002 with push belt CVT. Vehicle specifications for engine and transmission can be found in **table 1**.

Nissan Murano			
<i>Engine</i>		<i>Transmission</i>	
Type	3.5 ltr V6	Torque convertor	Yes, T_c -factor of 2.0
Max. engine power	180+ kW / 240+ Hp at 6000 rpm	Transmission type	Push belt CVT
Max. engine torque	350 Nm at 4000 rpm	Belt type	30/12 new design
		Ratio coverage	5.4
		Max. belt torque	500+ Nm

Table 1: Drive line specification Nissan Murano with push belt CVT.

With an engine specification of 350 Nm/180+ kW and a torque convertor with a torque ratio T_c of 2.0, the Nissan Murano CVT presently is the belt CVT with the highest power and torque capacity.

9. Conclusions

1. Test results support the improved life hypothesis of push belt rings through optimised curling and crowning radii of the rings. The results show an improvement in life testing times of about 70%. More in general this can be interpreted as a considerable improvement in power density for the 24/9 and 30/12 belt designs.
2. Given the good results, the new settings have been implemented in a new belt design leading to a further power density increase of the push belt CVT. The first transmission with the new belt design is the new 350 Nm/180 kW Nissan Murano application where a new 30/12 push belt is used.
3. Pre-bending of push belt rings during production introduces residual stress in the ring material that helps to decrease ring stress caused by bending during variator operation. This allows a higher power density for the push belt.
4. For rings with rectangular cross-section a pre-bend factor $R_{\text{curl}}/R_{\text{min}} = 2$ theoretically leads to minimal tension stresses in the rings in case anticlastic effects are neglected.
5. In this paper a one-dimensional ring model is described for optimisation of the curling radius of the rings. The model takes the effects of crowning and anticlastic curvature into account.
6. Simulations using the new model on crowned ring cross-sections influenced by anticlastic curvature effects reveal that pre-bend factors increase and lead to values significantly larger than 2. Effectively leading to larger optimum curling and /or crowning radii.

References

- [1] Brandsma, A., van Lith, J., Hendriks, E., "Push belt CVT developments for high power applications", Proc. of CVT99, Eindhoven University of Technology 1999, pp.142-147.
- [2] Beitz, W., Küttner, K.-H., "Dubbel, Taschenbuch für den Maschinenbau", Springer Verlag, 1999, pp. C18-C19.
- [3] Sinha, U., Levinson, D., "Bending stress relaxation of AISI 1095 steel strip". Taken from: Young, W.B., "Residual stress in design, Process and materials selection", ASMI, 1987, pp. 37-47.
- [4] Horrocks, D., Johnson W., "On anticlastic curvature with special reference to plastic bending", Int. Journal of Mechanical Science, Vol. 9, pp. 835-861, 1967.